

**FASTER-III,
A GENERALIZED-GEOMETRY MONTE CARLO
COMPUTER PROGRAM FOR THE TRANSPORT OF
OF NEUTRONS AND GAMMA RAYS
VOLUME I - SUMMARY REPORT**

by

T. M. Jordan

prepared for

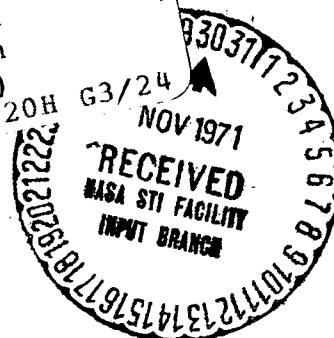
NATIONAL AERONAUTICS AND SPACE ADMINISTRATION

CONTRACT NAS3-14400

Reproduced by
**NATIONAL TECHNICAL
INFORMATION SERVICE**
Springfield, Va. 22151

DECEMBER 1970

N72-12682
Unclas
09796
(NASA-CR-124636) FASTER 3: A
GENERALIZED-GEOMETRY MONTE CARLO COMPUTER
PROGRAM FOR THE TRANSPORT OF T.M. Jordan
(ART Research Corp., Los Angeles, Calif.)
15 Dec. 1970 51-p CSCL 20H G3/24
OR IMX OR AD NUMBER) (CATEGORY)



A.R.T. RESEARCH CORPORATION

Dgt-65908R

FASTER-III,
A GENERALIZED-GEOMETRY
MONTE CARLO COMPUTER PROGRAM
FOR THE TRANSPORT OF
NEUTRONS AND GAMMA RAYS

VOLUME I - SUMMARY REPORT

by

Thomas M. Jordan

prepared for

NATIONAL AERONAUTICS AND SPACE ADMINISTRATION

December 15, 1970

CONTRACT NAS3-14400

Technical Management
NASA Lewis Research Center
Cleveland, Ohio
Millard L. Wohl

A.R.T. RESEARCH CORPORATION
1100 Glendon Avenue
Los Angeles, California 90024

~~PRECEDING PAGE BLANK NOT FILMED~~

PREFACE

This report was prepared by A.R.T. Research Corporation, Los Angeles, California, under Contract NAS3-14400 and was funded by the National Aeronautics and Space Administration-Lewis Research Center, Cleveland, Ohio. Inclusive dates of research were 24 June 1970 through 4 December 1970. The NASA Project Manager for this work was Mr. Millard L. Wohl.

This report comprises two (2) volumes; Volume I-Summary Report covers the theoretical basis for the FASTER-III computer program and results for sample problems; Volume II - Users Manual gives detailed operational instructions for the computer program.

PRECEDING PAGE BLANK NOT FILMED

ABSTRACT

This volume outlines the theory used in FASTER-III, a Monte Carlo computer program for the transport of neutrons and gamma rays in complex geometries. The program includes the treatment of geometric regions bounded by quadratic and quadric surfaces with multiple radiation sources which have a specified space, angle, and energy dependence. The program calculates, using importance sampling, the resulting number and energy fluxes at specified point, surface, and volume detectors. It has the additional capability of calculating the minimum weight shield configuration which will meet a specified dose rate constraint.

Results are presented for sample problems involving primary neutron and both primary and secondary photon transport in a spherical reactor-shield configuration. These results include the optimization of the shield configuration.

The users manual for the FASTER-III program is contained in a companion volume.

PRECEDING PAGE BLANK NOT FILMED

TABLE OF CONTENTS

<u>Section</u>		<u>Page</u>
1	INTRODUCTION AND SUMMARY	1
2	ANALYSIS	3
	2.1 Shield Dimension Derivatives	3
	2.2 Optimization Procedures	10
	2.3 Importance Parameter Optimization	14
3	SAMPLE PROBLEM RESULTS	23
4	CONCLUSIONS AND RECOMMENDATIONS	29
	REFERENCES	31

Appendix A-MONTE CARLO METHOD

PRECEDING PAGE BLANK NOT FILMED

LIST OF TABLES

<u>Table</u>		<u>Page</u>
1	SPHERICAL REACTOR-SHIELD CONFIGURATION	24
2	RESULTS OF BASE LINE CALCULATIONS AT 30 FEET FROM CORE CENTER	26
3	RESULTS OF SHIELD OPTIMIZATION	27

Section 1

INTRODUCTION AND SUMMARY

The original FASTER program, Reference 1, contained a number of new techniques which provided the capability of obtaining accurate radiation levels at specified points in complex geometries. The use of this program by NASA-Lewis Research Center and other Government facilities and contractors indicated the need to broaden the overall program capabilities, automate the importance sampling, increase the computational efficiency, and revise the users manual. This revised program has been designated FASTER-III to distinguish it from earlier versions.

A specific program capability developed for NASA-LeRC permits a calculation of minimum weight shield configurations for mobile nuclear reactor applications, e.g., nuclear propulsion for aircraft, surface effect vehicles, and space craft. The basic Monte Carlo transport method was extended to include a calculation of partial derivatives of the radiation fluxes with respect to specified shield dimensions. These derivatives are then used to define exponential relationships used in the shield optimization procedure. This optional program feature is described more completely in Section 2.

A number of program revisions had also been made by A.R.T. Research Corporation for various customers and to provide an internal capability for solving a variety of radiation transport problems. These revisions are included in the FASTER-III program. Particularly noteworthy are the following:

- (1) A calculation of optimal importance sampling parameters based on partial derivatives of the variance (Section 2.3).

- (2) The acceptance of data in either fixed or variable field formats including the ANISN-DTF format for neutron cross sections.
- (3) The calculation of time-dependent neutron and photon transport (using time moments and/or time intervals) including an optional exponential atmosphere.
- (4) The improvement and addition of importance sampling models with the various importance sampling parameters built into the program.

Various program features are described in References 2-6.

The application of the FASTER-III program to a shield optimization problem is discussed in Section 3. The problem involved a spherical reactor-shield configuration and included primary neutrons and both primary and secondary photons. Conclusions and recommendations are presented in Section 4.

Volume II (Users Manual) presents the detailed description of the FASTER-III program along with all the instructions for operation on the IBM 7094, UNIVAC 1108, CDC 6600, and IBM 360-0S (single or double precision) computers.

Section 2

ANALYSIS

The techniques used in calculating optimum shield configurations and optimum importance sampling parameters are summarized below. The discussion is given in three parts: derivatives of fluxes with respect to shield dimensions, optimization techniques, and derivatives of variance with respect to importance sampling parameters. The basic Monte Carlo techniques assumed in this discussion are summarized in Appendix A.

2.1 Shield Dimension Derivatives

The dose rate at a point detector \underline{y} for a specified reactor shield configuration is written as:

$$D(\underline{y}) = \sum_{j=1}^J R_j \phi_j(\underline{y}) \quad (1)$$

where J is the total number of energy groups for both neutrons and photons (including secondaries), $\phi_j(\underline{y})$ is the particle flux in the j th energy group, and R_j is the conversion factor from flux to dose rate. The rate of change of the dose rate with respect to a shield dimension is simply

$$\frac{\partial D(\underline{y})}{\partial t_\ell} = \sum_{j=1}^J R_j \frac{\partial \phi_j}{\partial t_\ell}(\underline{y}) \quad \ell = 1, 2, \dots, L \quad (2)$$

where L is the total number of shield dimensions and t_ℓ is the value of the ℓ th shield dimension.

The equation used by the program for determining the flux is written as:

$$\phi_j(\underline{y}) = \frac{1}{N} \sum_{n=1}^N \sum_k S_{jkn}^*(\underline{u}_{kn}) K_j(\underline{z}_{kn}, \underline{y}), \quad \underline{u}_{kn} = \frac{\underline{y} - \underline{z}_{kn}}{|\underline{y} - \underline{z}_{kn}|} \quad (3)$$

where N is the total number of histories tracked via the Monte Carlo method, k is the number of particle collisions, \underline{z}_{kn} is the position of the k th collision of the n th history, $S_{jkn}^*(\underline{u}_{kn})$ the number of particles in the j th energy group emerging from \underline{z}_{kn} in the direction \underline{u}_{kn} of the detector per unit solid angle, and $K_j(\underline{z}_{kn}, \underline{y})$ represents the material and geometric attenuation kernel for particles in the j th energy group going from \underline{z}_{kn} to the detector.

The partial derivative of the flux with respect to a shield dimension is simply:

$$\frac{\partial \phi_j(\underline{y})}{\partial t_\ell} = \frac{1}{N} \sum_{n=1}^N \sum_k \frac{\partial}{\partial t_\ell} \left[S_{jkn}^*(\underline{u}_{kn}) K_j(\underline{z}_{kn}, \underline{y}) \right] \quad (4)$$

The summations are a minor part of the calculation. Therefore, the notation is simplified by concentrating on the elements in the summation

$$\frac{\partial \theta_{jkn}}{\partial t_\ell} = \frac{\partial}{\partial t_\ell} \left[S_{jkn}^*(\underline{u}_{kn}) K_j(\underline{z}_{kn}, \underline{y}) \right] \quad (5)$$

where θ_{jkn} represents the contribution to the flux in the j th energy group from the k th collision of the n th history.

This equation is rewritten as

$$\begin{aligned} \frac{\partial \theta_{jkn}}{\partial t_\ell} &= \theta_{jkn} \frac{\partial}{\partial t_\ell} \ln \left[S_{jkn}^*(u_{kn}) K_j(z_{kn}, y) \right] \\ &= \theta_{jkn} \left[\frac{\partial}{\partial t_\ell} \ln S_{jkn}^*(u_{kn}) + \frac{\partial}{\partial t_\ell} \ln K_j(z_{kn}, y) \right] \end{aligned} \quad (6)$$

The second term in brackets involves the attenuation kernel

$$K_j(z_{kn}, y) = \frac{\exp \left[- \sum_{m=1}^M s_m \sigma_{jm} \right]}{s^2} \quad (7)$$

where M is the total number of regions traversed from z_{kn} to the detector, s_m is the path length for the m th region traversed, σ_{jm} is the total cross section of this region for particles in the j th energy group, and s is the total distance from z_{kn} to the detector, i.e.,

$$s = \sum_{m=1}^M s_m \quad (8)$$

A substitution of this kernel gives:

$$\begin{aligned} \frac{\partial}{\partial t_\ell} \ln K_j(z_{kn}, x) &= \frac{\partial}{\partial t_\ell} \left[- \sum_{m=1}^M s_m \sigma_{jm} - 2 \ln \sum_{m=1}^M s_m \right] \\ &= - \sum_{m=1}^M \sigma_{jm} \frac{\partial s_m}{\partial t_\ell} - \frac{2 \sum_{m=1}^M \frac{\partial s_m}{\partial t_\ell}}{\sum_{m=1}^M s_m} \\ &= - \sum_{m=1}^M \left(\sigma_{jm} + \frac{2}{s} \right) \frac{\partial s_m}{\partial t_\ell} \end{aligned} \quad (9)$$

The partial derivative of the partial path length s_m with respect to the shield dimension t_ℓ is zero unless the m th region traversed is affected by a change in t_ℓ . In particular, if t_ℓ is a characteristic dimension of the region, i.e., its thickness, then

$$\frac{\partial s_m}{\partial t_\ell} = \frac{1}{\mu_{knm}} \quad , \quad \mu_{knm} = \underline{u}_{kn} \cdot \underline{n}_{knm} \quad (10)$$

where μ_{knm} is the cosine of the angle measured from the surface normal \underline{n}_{knm} , with which the particle crosses the boundary of the region.

In the strict sense, the change of the dimension of one shield region can affect other shield regions. In particular, for a spherically symmetric reactor-shield configuration, an increase in the thickness of a shield region forces a movement of all shield regions having a larger radius. The inclusion of these effects in the above equation unnecessarily complicates the analysis and the calculations. The primary effect of changing a shield region dimension is to change the number of mean free paths which particles have to traverse in reaching the detector. Therefore, in calculating the derivatives, only the effect of the material attenuation is treated.

The derivatives at a specific boundary crossing m' then simplify to:

$$\begin{aligned} \frac{\partial}{\partial t_\ell} \ln K_j(\underline{z}_{kn}, \underline{y}) &= - \sum_{m=1}^M (\sigma_{jm} + \frac{2}{s}) \frac{\partial s_m}{\partial t_\ell} \\ &= - (\sigma_{jm'} + \frac{2}{s}) \frac{1}{\mu_{knm'}} - (0 + \frac{2}{s}) \frac{1}{-\mu_{knm'}} \\ &= \sigma_{jm'} / \mu_{knm'} \end{aligned} \quad (11)$$

where m' is the index of a region having t_ℓ as a dimension.

The partial derivatives of the particle weight with respect to the shield dimensions -- the first term in brackets in equation 6 -- are zero at the point of origin of all primary particles. For subsequent particle collisions, the derivatives are calculated using the relationship between particle weights on subsequent collisions:

$$S_{jkn}^*(\underline{u}_{kn}) = \frac{\sum_i S_{i,k-1,n}^*(\underline{v}_{kn}) K_i(z_{k-1,n}, z_{kn}) T_{ij}(z_{kn}, \underline{v}_{kn} \cdot \underline{u}_{kn})}{p_{kn}^*(z_{kn})}$$

$$\underline{v}_{kn} = \frac{z_{kn} - z_{k-1,n}}{|z_{kn} - z_{k-1,n}|} \quad (12)$$

where $S_{i,k-1,n}^*(\underline{v}_{kn})$ is the number of particles coming out of the previous collision point in the direction \underline{v}_{kn} and in the i th energy group, $K_i(z_{k-1,n}, z_{kn})$ is the attenuation kernel between particle collision points, $T_{ij}(z_{kn}, \underline{v}_{kn} \cdot \underline{u}_{kn})$ is the scattering kernel for transfer of particles from group i to group j , and $p_{kn}^*(z_{kn})$ is the probability density function used in selecting the collision point.

A straightforward substitution gives

$$\frac{\partial}{\partial t_\ell} \ln S_{jkn}^*(\underline{u}_{kn}) = \frac{\partial}{\partial t_\ell} \ln \left[\frac{\sum_i S_{i,k-1,n}^*(\underline{v}_{kn}) K_i(z_{k-1,n}, z_{kn}) T_{ij}(z_{kn}, \underline{v}_{kn} \cdot \underline{u}_{kn})}{p_{kn}^*(z_{kn})} \right] \quad (13)$$

After some manipulation, this reduces to

$$\frac{\partial}{\partial t_\ell} \ln S_{jkn}^*(u_{kn}) = \frac{1}{S_{jkn}^*(u_{kn})} \sum_i V_{ijkln} \left[\frac{\partial}{\partial t_\ell} \ln S_{i,k-1,n}^*(v_{kn}) + \frac{\partial}{\partial t_\ell} \ln K_i(z_{k-1,n}, z_{kn}) - \frac{\partial}{\partial t_\ell} \ln p_{kn}^*(z_{kn}) \right] \quad (14)$$

where

$$V_{ijkln} = \frac{S_{i,k-1,n}^*(v_{kn}) K_i(z_{k-1,n}, z_{kn}) T_{ij}(z_{kn}, v_{kn}, u_{kn})}{p_{kn}^*(z_{kn})} \quad (15)$$

The first term in brackets in equation 14 is the same partial derivative for collision k-1 as the partial derivative now being calculated for collision k. Therefore, it is known, either identically zero for k=0, or as determined from equation 14 for k>0. The second term in brackets in equation 14 is similar to the second term in brackets in equation 6 and is therefore determined by equation 11. The last term in brackets involves the definition of the probability density function used to select the collision point z_{kn} .

The probability density function for a collision point has the form

$$p_{kn}^*(z_{kn}) = a_{kn}^*(v_{kn}) \frac{A(s)a(s) \exp \left[-\int_0^s a(s') ds' \right]}{\int_0^\infty A(s')a(s') \exp \left[-\int_0^{s'} a(s'') ds'' \right] ds'} \quad (16)$$

where $q_{kn}^*(v_{kn})$ is a probability density function used to select the particle direction, $s = |z_{kn} - z_{k-1,n}|$ is the distance of the selected collision point z_{kn} from the previous collision point, $A(s)$ is an importance factor for each region which changes discontinuously at region boundaries, and $a(s)$ is an effective cross section which changes discontinuously at region boundaries and which may change continuously within a region.

The derivative of the logarithm of $p_{kn}^*(z_{kn})$ involves only those terms which change when a shield dimension changes, i.e.,

$$\frac{\partial}{\partial t_\ell} \ln p_{kn}^*(z_{kn}) = \frac{\partial}{\partial t_\ell} \left[-\int_0^s a(s') ds' \right] - \frac{\partial}{\partial t_\ell} \ln \left[\int_0^\infty A(s') a(s') \exp \left[-\int_0^{s'} a(s'') ds'' \right] ds' \right] \quad (17)$$

Let s_ℓ denote the distance to a boundary involving the ℓ th shield dimension. If the first term on the left side of equation 17 is affected by a change in this shield dimension, i.e. if $s > s_\ell$, then

$$\begin{aligned} \frac{\partial}{\partial t_\ell} \left[-\int_0^s a(s') ds' \right] &= -a(s_\ell) \frac{\partial s_\ell}{\partial t_\ell} \\ &= -a(s_\ell) \frac{1}{\mu_{\ell kn}} \end{aligned} \quad (18)$$

where $a(s_\ell)$ is the effective cross section at the boundary of the shield and $\mu_{\ell kn}$ is the cosine the particle path makes with the outer shield normal. If there is any crossing involving the ℓ th shield dimension, the second term in equation 18 will always have a non-zero derivative, i.e.,

$$\frac{\partial}{\partial t_l} \ln \left[\int_0^\infty A(s') a(s') \exp \left[- \int_0^{s'} a(s'') ds'' \right] \right]$$

$$= \frac{A(s_l) a(s_l) \frac{1}{\mu_{lkn}} \exp \left[- \int_0^{s_l} a(s') ds' \right]}{\int_0^\infty A(s') a(s') \exp \left[- \int_0^{s'} a(s'') ds'' \right] ds'} \quad (19)$$

Curved shield surfaces may be crossed more than once along the path between two particle collision points. Therefore, a summation of equations 18 and 19 over every intersection involving the l th shield dimension is required to completely evaluate equation 17.

2.2 Optimization Procedures

The shield optimization calculation yields the set of shield dimensions $\underline{t}' = (t'_1, t'_2, \dots, t'_l, \dots, t'_L)$ such that the dose rate, $D(\underline{t}')$, meets the dose constraint. The Monte Carlo calculation is performed for an initial set of shield dimensions $\underline{t} = (t_1, t_2, \dots, t_l, \dots, t_L)$ and yields a set of fluxes, $\phi_j(\underline{t})$, $j = 1, 2, \dots, J$ and derivatives, $\frac{\partial \phi_j(\underline{t})}{\partial t_l}$, $j = 1, 2, \dots, J$; $l = 1, 2, \dots, L$. The assumption is made that the fluxes vary exponentially with respect to shield dimension changes in the form

$$\phi_j(\underline{t}') = \phi_j(\underline{t}) \exp \left[\underline{a}_j \cdot (\underline{t}' - \underline{t}) \right] \quad (20)$$

where $\underline{a}_j = (a_{j1}, a_{j2}, \dots, a_{jL})$. It follows that

$$\begin{aligned} \frac{\partial \phi_j(\underline{t})}{\partial t'_\ell} &= \phi_j(\underline{t}) \exp\left[\underline{a}_j \cdot (\underline{t}' - \underline{t})\right] \frac{\partial}{\partial t'_\ell} \left[\underline{a}_j \cdot (\underline{t}' - \underline{t})\right] \\ &= \phi_j(\underline{t}') a_{j\ell} \end{aligned} \quad (21)$$

In particular

$$\frac{\partial \phi_j(\underline{t})}{\partial t'_\ell} = a_{j\ell} \phi_j(\underline{t}) \quad (22)$$

or

$$a_{j\ell} = \frac{\partial \phi_j(\underline{t})}{\partial t'_\ell} / \phi_j(\underline{t}) \quad (23)$$

The weight is also expressed as a function of the shield dimensions. The weight is denoted by $W(t')$ and for spherically symmetric shields:

$$\begin{aligned} W(t') &= \frac{4\pi}{3} \left\{ \rho_1 \left[(r_0 + t'_1)^3 - r_0^3 \right] + \rho_2 \left[(r_0 + t'_1 + t'_2)^3 - (r_0 + t'_1)^3 \right] + \dots \right\} \\ &= \frac{4\pi}{3} \sum_{\ell=1}^L \rho_\ell \left\{ (r_0 + \sum_{m=1}^{\ell} t'_m)^3 - (r_0 + \sum_{m=1}^{\ell-1} t'_m)^3 \right\} \end{aligned} \quad (24)$$

where ρ_l is the density of the l th shield region and r_0 is the minimum shield radius.

The purpose of the optimization procedure is to minimize the weight $W(\underline{t}')$ subject to the dose rate constraint $D(\underline{t}') = D_0$ where D_0 is a specified dose rate. At this optimum, the following equalities hold

$$Q_l = \frac{\frac{\partial D(\underline{t}')}{\partial t'_l}}{\frac{\partial W(\underline{t}')}{\partial t'_l}} = \text{constant}, \quad l = 1, 2, \dots, L$$

The necessary derivatives are:

$$\frac{\partial D(\underline{t}')}{\partial t'_l} = \sum_{j=1}^J R_j \frac{\partial \phi_j(\underline{t}')}{\partial t'_l} = \sum_{j=1}^J R_j a_{jl} \phi_j(\underline{t}) \exp \left[\underline{a}_j \cdot (\underline{t}' - \underline{t}) \right] \quad (26)$$

and for spherically symmetric shield:

$$\frac{\partial W(\underline{t}')}{\partial t'_l} = 4\pi \sum_{i=l}^L \rho_j \left[(r_0 + \sum_{m=1}^i t'_m)^2 - (r_0 + \sum_{m=1}^{i-1} t'_m)^2 \right] \quad (27)$$

In arriving at the optimum shield, the total shield weight is built up in increments of weight ΔW . Each increment in shield weight is always associated with a particular shield dimension. At each iteration, the particular shield dimension is selected by examining the values of the shield weight quality factors, Q_l . Each factor Q_l represents the approximate change

in dose rate per unit change in weight corresponding to a change in the l th shield dimension. Negative Q_l 's are the most usual and correspond to shields for which an increase in weight -- and shield dimensions -- gives a decrease in dose rate. Positive Q_l 's can occur, however, and correspond to shields for which an increase in weight also increases the dose rate.

If, at a particular iteration, the dose rate is above the dose rate constraint, the minimum shield weight increment would correspond to the least positive value of those Q_l 's for which $Q_l > 0$ and for which $t'_l > t_l(\text{min})$, where $t_l(\text{min})$ is the minimum value of the l th shield dimension. If such a Q_l exists, the dose rate can be decreased while also decreasing the shield weight the maximum amount. If there isn't such a Q_l , the next best procedure is to find the most negative of the Q_l 's for which $Q_l < 0$ and for which $t'_l < t_l(\text{max})$, where $t_l(\text{max})$ is the maximum value of the l th shield dimension. A change in that Q_l would give the maximum decrease in dose rate per unit increase in weight.

If the dose rate is below the specified dose rate at a particular iteration, the minimum shield weight increment would correspond to the least negative of those Q_l 's for which $Q_l < 0$ and for which $t'_l > t_l(\text{min})$. If such a Q_l exists, the dose rate can be increased while decreasing the shield weight the maximum amount. If there isn't such a Q_l , the next best procedure is to find the most positive of those Q_l 's for which $Q_l > 0$ and for which $t'_l < t_l(\text{max})$. A change in that Q_l would give the maximum increase in dose rate per unit increase in weight.

Assuming a particular value Q_m of the Q_l 's is selected through the above arguments, the corresponding shield dimension t'_m is changed by a maximum amount Δt_m where Δt_m is calculated as

$$\Delta t_m = \frac{\Delta W}{\frac{\partial W}{\partial t'_l}(t'_l)} \quad (28)$$

If this change would put t'_m outside one of its specified limits, the value of t'_m would be set to that limit, i.e., $t'_m(\min) \leq t'_m \leq t'_m(\max)$. The shield weight increment ΔW is calculated as

$$\Delta W = \frac{D_o - D(t'_m)}{Q_m} \quad (29)$$

subject to the constraint that $|\Delta W| < \Delta W_o$ where ΔW_o is a specified maximum shield weight increment per iteration. Note that ΔW , and therefore Δt_m , may be positive or negative depending on the value of Q_m and whether the dose rate is above or below the dose rate constraint.

Once a shield dimension is changed, the dose, weight, and their derivatives are re-evaluated and the entire process is repeated. The optimization would be discontinued in several ways. If the dose rate equals the dose rate constraint within the relative error of the original Monte Carlo dose rate calculation, the program will proceed to the next problem -- which may be identical except with more histories to tighten the convergence of Monte Carlo calculations. Similarly, if all shield dimensions have reached their minimum or maximum values, and if the optimum shield cannot be determined with these constraints, the program would again proceed to the next problem. Finally, if the dose rate and dose rate constraint are decades apart in value, the program would reevaluate the fluxes and their derivatives by Monte Carlo every time the dose rate changed by more than a specified factor during the optimization procedure.

2.3 Importance Parameter Optimization

The optimization of the importance sampling must be performed for some function, e.g., dose rate, of the energy-dependent

fluxes since there is a different optimum for every initial particle energy. Therefore, assume that a minimum variance calculation of the dose rate is required where

$$\bar{D}_N = \frac{1}{N} \sum_{n=1}^N D_n \quad (30)$$

where N is the total number of histories and D_n is the dose rate from the n th history and \bar{D}_N is the average value of the dose rate after N histories. The relative error of this dose rate is given by

$$E_N = \frac{1}{\bar{D}_N} \left\{ \frac{1}{N^2} \left[\sum_{n=1}^N D_n^2 - N \bar{D}_N^2 \right] \right\}^{\frac{1}{2}} \quad (31)$$

Taking the logarithm of this equation and then performing a formal calculation of the partial derivative with respect to an unspecified parameter a yields

$$\begin{aligned} \frac{\partial}{\partial a} \ln E_N &= - \frac{\partial}{\partial a} \ln \bar{D}_N - \frac{\partial}{\partial a} \ln N + \frac{1}{2} \frac{\partial}{\partial a} \ln \left[\sum_{n=1}^N D_n^2 - N \bar{D}_N^2 \right] \\ &= - \frac{\frac{\partial}{\partial a} \bar{D}_N}{\bar{D}_N} + \frac{\sum_{n=1}^N D_n \frac{\partial D_n}{\partial a} - N \bar{D}_N^2 \frac{\partial \bar{D}_N}{\partial a}}{\sum_{n=1}^N D_n^2 - N \bar{D}_N^2} \\ &= \frac{1}{N^2 \bar{D}_N^3 E_N^2} \left[\bar{D}_N \sum_{n=1}^N D_n \frac{\partial D_n}{\partial a} - \left(\sum_{n=1}^N D_n^2 \right) \frac{\partial \bar{D}_N}{\partial a} \right] \quad (32) \end{aligned}$$

Thus the partial derivative of the relative error with respect to the parameter a is:

$$\frac{\partial E_N}{\partial a} = \frac{1}{N^2 \bar{D}_N^3 E_N} \left[\bar{D}_N \sum_{n=1}^N D_n \frac{\partial D_n}{\partial a} - \left(\sum_{n=1}^N D_n^2 \right) \frac{\partial \bar{D}_N}{\partial a} \right] \quad (33)$$

The dose rate from the n th history is given by

$$D_n = \sum_{j=1}^J R_j \sum_k \phi_{jkn} \quad (34)$$

where J is the total number of energy groups, k is the number of particle collisions, R_j is the flux to dose rate conversion factor for the j th energy group, and ϕ_{jkn} is the flux in the j th group from the k th collision of the n th history. Since

$$\frac{\partial \bar{D}_N}{\partial a} = \frac{1}{N} \sum_{n=1}^N \frac{\partial D_n}{\partial a}, \quad (35)$$

the calculations required to evaluate equation 33 all involve the summation of terms which involve

$$\frac{\partial D_n}{\partial a} = \frac{\partial}{\partial a} \sum_{j=1}^J \left(R_j \sum_k \phi_{jkn} \right) = \sum_{j=1}^J R_j \sum_k \frac{\partial \phi_{jkn}}{\partial a} \quad (36)$$

The remainder of the analysis, therefore, can be concentrated on the partial derivatives of the fluxes. All other operations which must be performed are given above.

The fluxes typically depend on the detector position \underline{y} , so the equation for the particle flux is written as

$$\phi_{jkn}(\underline{y}) = S_{jkn}^*(\underline{u}_{kn}) K_j(\underline{z}_{kn}, \underline{y}) \quad (37)$$

The transport kernel $K_j(\underline{z}_{kn}, \underline{y})$ does not involve any importance sampling parameters so that

$$\frac{\partial \phi_{jkn}(\underline{y})}{\partial a} = \frac{\partial S_{jkn}^*(\underline{u}_{kn})}{\partial a} K_j(\underline{z}_{kn}, \underline{y}) \quad (38)$$

This equation can also be written as

$$\frac{\partial \phi_{jkn}(\underline{y})}{\partial a} = S_{jkn}^*(\underline{u}_{kn}) K_j(\underline{z}_{kn}, \underline{y}) \frac{\partial}{\partial a} \ln S_{jkn}^*(\underline{u}_{kn}) \quad (39)$$

Without going into great detail, it turns out that the particle weight $S_{jkn}^*(\underline{u}_{kn})$ is composed of a purely analytical numerator, $V_{jkn}(\underline{u}_{kn})$ and a denominator which is the product of all the probability density functions used to select the collision points, i.e.,

$$S_{jkn}^*(\underline{u}_{kn}) = \frac{V_{jkn}(\underline{u}_{kn})}{\prod_{\ell=0}^k p_{\ell n}^*(\underline{z}_{\ell n})} \quad (40)$$

Therefore

$$\ln S_{jkn}^*(\underline{u}_{kn}) = \ln V_{jkn}(\underline{u}_{kn}) - \ln \prod_{\ell=0}^k p_{\ell n}^*(\underline{z}_{\ell n}) \quad (41)$$

Since $V_{jkn}(u_{kn})$ does not explicitly involve any importance parameters, it follows that

$$\begin{aligned} \frac{\partial}{\partial a} \ln S_{jkn}^*(u_{kn}) &= - \frac{\partial}{\partial a} \ln \prod_{\ell=0}^k p_{\ell n}^*(z_{\ell n}) \\ &= - \sum_{\ell=0}^k \frac{\partial}{\partial a} \ln p_{\ell n}^*(z_{\ell n}) \end{aligned} \quad (42)$$

Therefore, equation 39 can be re-written as

$$\frac{\partial \phi_{jkn}}{\partial a}(\underline{y}) = - \phi_{jkn}(\underline{y}) \sum_{\ell=0}^k \frac{\partial}{\partial a} \ln p_{\ell n}^*(z_{\ell n}) \quad (43)$$

Moreover, the partial derivatives are energy-independent so that equation 36 becomes

$$\frac{\partial D_n}{\partial a} = \sum_k \left(\sum_{j=1}^J R_j \phi_{jkn}(\underline{y}) \right) \left(- \sum_{\ell=0}^k \frac{\partial}{\partial a} \ln p_{\ell n}^*(z_{\ell n}) \right) \quad (44)$$

The evaluation of the partial derivatives of the probability density functions can be written as

$$\sum_{\ell=1}^k \frac{\partial}{\partial a} \ln p_{\ell n}^*(z_{\ell n}) = \sum_{\ell=0}^{k-1} \frac{\partial}{\partial a} \ln p_{\ell n}^*(z_{\ell n}) + \frac{\partial}{\partial a} \ln p_{kn}^*(z_{kn}) \quad (45)$$

At the k th collision, the first term on the left side of equation 45 is known, identically zero if $k=0$. Therefore, the analysis is completed after examining the calculation of the second term.

At this point it is necessary to identify the particular importance parameter a . Since most of the importance sampling parameters have fairly involved roles, the technique will be applied here to a set of parameters which can have a reasonably simple role. These parameters consists of the relative importance I_r of each region. Normally these parameters are all equal. However, in asymmetric problems, it turns out that some regions are much more important in terms of their scattering contributions to a detector. Therefore, these important regions have a larger value of I_r .

The region importance enters into the selection of a collision point through the following probability density function:

$$p_{kn}^*(z_{kn}) = \frac{I_r p_r^*(s)}{\sum_{h=1}^H I_h P_h^*} \quad (46)$$

where r is the region in which the collision occurs (selected at random), $p_r^*(s)$ is the piecewise continuous probability density function in this region at the selected collision point (a distance s from the previous collision point), H is the total number of regions in which the collision could have occurred, and P_h^* is the integral of $p_h^*(s')$ over the partial path length in region h .

Calculating the logarithm of each side of the equation yields:

$$\ln p_{kn}^*(z_{kn}) = \ln I_r + \ln p_r^*(s) - \ln \sum_{h=1}^H I_h P_h^* \quad (47)$$

The partial derivative of equation 47 with respect to the specific importance parameter I_g -- the relative importance of region g -- yields

$$\frac{\partial}{\partial I_g} \ln p_{km}^*(z_{km}) = \frac{1}{I_r} \delta_{gr} - \frac{\sum_{h=1}^H P_h^* \delta_{gh}}{\sum_{h=1}^H I_h P_h^*} \quad (48)$$

where $\delta_{gh} = 0$ if region h is not region g and $\delta_{gg} = 1$.

Thus equation 48 is evaluated during the random selection of the k th collision point and the final term necessary to evaluate equation 45 and all preceding equations has been determined.

The above analysis is used to calculate the partial derivatives of the relative error of the dose rate with respect to the relative importance I_r of each geometric region, and a similar analysis is performed for the other importance sampling parameters. The result of the complete Monte Carlo calculation is a set of partial derivatives which, for the region importance, are given by

$$\frac{\partial E_N}{\partial I_r} = \frac{1}{N^2 \bar{D}_N^3 E_N} \left[\bar{D}_N \sum_{n=1}^N D_n \frac{\partial D_n}{\partial I_r} - \left(\sum_{n=1}^N D_n^2 \right) \frac{1}{N} \sum_{n=1}^N \frac{\partial D_n}{\partial I_r} \right] \quad (49)$$

where $\frac{\partial D_n}{\partial I_r}$ is obtained from equation 44 using equations 45 and 48.

After the calculation is completed, optimal values of the importance sampling parameters are calculated by requiring that the relative error be zero--not actually achieved of course.

By a first order expansion

$$E'_N = 0 = E_N + \sum_{r=1}^R \frac{\partial E_N}{\partial I_r} (I'_r - I_r) \quad (50)$$

where R is the total number of regions. A simple gradient analysis says that $I'_r - I_r$ should be proportional to $\frac{\partial E_N}{\partial I_r}$ so that

$$I'_r = I_r + C \frac{\partial E_N}{\partial I_r} \quad (51)$$

where, by substitution into equation 50,

$$C = \frac{-E_N}{\sum_{r=1}^R \left(\frac{\partial E_N}{\partial I_r} \right)^2} \quad (52)$$

The program prints the optimum values of I'_r and other importance parameters after completing the Monte Carlo flux calculation. This analysis is performed for every response function. After more experience is obtained with the technique, the program could be modified to change these parameters internally corresponding to a specified response function.

Section 3

SAMPLE PROBLEM RESULTS

Two problems were investigated using the shield optimization capabilities of the FASTER-III program. Both problems involved a spherical reactor-shield configuration and included primary neutrons and both primary and secondary photons.

The two problems were similar except for the power level, 375 MW and 600 MW respectively. Both problems used a flat radial distribution for the primary neutron and photon source distribution. The primary photon source included an infinite operation equilibrium fission product term.

The core radii for the two problems were 82.38 and 96.38 cm respectively, corresponding to a power density of 4.53 MW/ft³. Following the core was a 7.62 cm Be reflector; a 5 cm depleted uranium shield; three depleted uranium-borated water shields of 57, 15, and 15 cm thickness and 6.4, 4.6, and 2.8 gm/cm³ density respectively; and a 117 cm borated water shield. This base line shield configuration was based on parameters obtained from SANE-SAGE calculations and subsequent calculations using the UNAMIT program, Reference 7. The reactor-shield compositions are given in Table 1.

The primary neutron transport calculation utilized multigroup cross sections for 26 energy groups. Fifteen energy groups were utilized for both primary and secondary photons. The secondary production cross sections included both inelastic and capture gammas.

These initial configurations were each analyzed for a point detector 30 feet from the core center by following approximately

TABLE 1

SPHERICAL REACTOR-SHIELD CONFIGURATION

Element	COMPOSITIONS (10^{24} atoms/cm ³)						
	CORE	REFLECTOR	U ²³⁸ SHIELD	MIX 1 SHIELD	MIX 2 SHIELD	MIX 3 SHIELD	H ₂ O+B SHIELD
H	0.01976	0.0	0.0	0.0451	0.0516	0.0580	0.0645
Be ⁹	0.0	0.120	0.0	0.0226	0.0258	0.0290	0.0337
B	0.0	0.0	0.0	0.000671	0.000766	0.000862	0.000958
O	0.01184	0.0	0.0	0.0	0.0	0.0	0.0
Al	0.0512	0.0	0.0	0.0	0.0	0.0	0.0
Zr	0.01744	0.0	0.0	0.0	0.0	0.0	0.0
U ²³⁵	0.000979	0.0	0.0	0.0	0.0	0.0	0.0
U ²³⁸	0.000078	0.0	0.0482	0.01446	0.00964	0.00482	0.0

500 energy-dependent packets of primary neutrons and photons and approximately 7000 packets of secondary photons. The dose rates obtained from these calculations are tabulated in Table 2 including a breakdown by secondary source region. Each of these problems required about 28 minutes on the UNIVAC 1108 computer.

The basic calculated dose rates and dose rate derivatives were also used by the FASTER-III program to calculate the minimum weight shield configuration which would give a dose rate of 0.25 mr/hr at the specified detector point. The final shield configurations following the optimization are given in Table 3.

In both cases, the optimum shield configuration is significantly different than the base line configuration. Since the base line configuration was not generated by the FASTER-III program it is difficult to discuss many factors entering into that calculation which would account for the different optimal configuration. It is noted, however, that the base line configuration was generated using parameters corresponding to a calculated dose rate an order of magnitude below the specified dose rate constraint, Reference 8. As such, the base line configuration used in the FASTER-III program was determined from an extrapolation of a different base line configuration.

A more critical critique can be made of the FASTER-III results independently. First it is noted that neither problem saw a significant contribution from photon sources in the core region. In fact, the 600 MW reactor dose rate from this source was about a factor of two less than it was for the 375 MW reactor. This difference is ascribed to the problem statistics since core photon sources see approximately 30 mean free paths of shield material. Therefore, it is doubtful if this dose rate component is converged even with a factor of two after only 500 packets.

TABLE 2

RESULTS OF BASE LINE CALCULATIONS
AT 30 FEET FROM CORE CENTER

<u>DOSE RATE COMPONENT</u>	<u>375 MW REACTOR (mr/hr)</u>	<u>600 MW REACTOR (mr/hr)</u>
Photon Source Region		
Core	0.009	0.004
Reflector	3.5×10^{-6}	6.3×10^{-6}
Depleted Uranium	3.2×10^{-5}	1.3×10^{-5}
Mix 1 Shield	0.018	0.026
Mix 2 Shield	0.062	0.075
Mix 3 Shield	0.017	0.063
Borated Water Shield	0.011	0.022
Total Photons	0.120 ± 0.034	0.187 ± 0.054
Neutrons	0.020 ± 0.002	0.027 ± 0.003
Total	0.140	0.214

TABLE 3

RESULTS OF SHIELD OPTIMIZATION
(0.25 mr/hr at 30 feet)

Quantity	375 MW		600 MW	
	REACTOR		REACTOR	
	Initial	Final	Initial	Final
Dose Rate (mr/hr)				
Photon	0.120	0.126	0.187	0.153
Neutron	<u>0.020</u>	<u>0.124</u>	<u>0.027</u>	<u>0.097</u>
Total	0.140	0.250	0.214	0.250
Shield Weight (10^3 kg)				
Depleted U	10.2	12.6	13.8	0.0
Mix 1	71.2	0.0	89.2	6.6
Mix 2	22.1	52.4	26.4	52.4
Mix 3	16.1	12.2	19.0	63.1
Water	<u>86.7</u>	<u>80.3</u>	<u>97.7</u>	<u>85.3</u>
Total	206.3	157.5	246.1	207.4
Shield Thickness (cm)				
Depleted U	5.0	6.1	5.0	0.0
Mix 1	57.0	0.0	57.0	7.0
Mix 2	15.0	57.3	15.0	48.4
Mix 3	15.0	13.5	15.0	51.4
Water	117.0	120.8	117.0	98.4

The small contribution from core photon sources decreases the amount of high Z shields required around the core. Therefore, both problems gave a significant change in the first two shield dimensions during the optimization. In the 375 MW problem, the first mixture of depleted uranium-borated water ($\rho = 6.4 \text{ gm/cm}^3$) was eliminated entirely. In the 600 MW problem, the depleted uranium and most of the first mixture were eliminated.

The main difference between the two FASTER-III calculations was the shift in the placement of lighter shield mixes towards the core for the 600 MW problem. An examination of the secondary photon dose components indicates that the contribution from the outer two shields was about 25% for the 375 MW reactor and almost 50% for the 600 MW reactor. Since these sources depend on the neutron attenuation through the closer regions and since lower effective Z materials are better neutron attenuators on a weight basis, the 600 MW problem tends to replace high effective Z material with a lower effective Z material.

The differences in the contribution from secondary sources in the outer shield regions is greater than expected for the nominal difference in the core region. Therefore, much of the difference in these sources must be ascribed to statistical variations. In fact, both problems had approximately 25-30% calculated relative error in the total photon dose rate. It should be noted that the FASTER-III program includes a number of importance sampling techniques which could be used to decrease this error. However, both problems were run using the built-in definitions of importance parameters. Alternatively, more histories could have been used although the computer time requirements would have become excessive.

Section 4

CONCLUSIONS AND RECOMMENDATIONS

The FASTER-III program was developed to calculate neutron and photon fluxes at specified points in complex geometries. Alternatively, it can also calculate fluxes averaged over specified surfaces and volumes. The program was designed such that data preparation is simple and so that very little judgment is required to set up the importance sampling for most problems. The FASTER-III program satisfies these requirements very well.

The shield weight optimization capability included in the FASTER-III program permits the calculation of both base line radiation levels and optimal shield thicknesses all in a single computer run. However, the very large attenuation factors involved in the demonstration problems yielded some questionable results. In particular, the statistical differences in the relative contribution from various secondary source regions caused corresponding variations in the relative distributions of shield materials. Of course the statistical variations would be less in problems with less overall attenuation.

The effect of statistical differences on the shield optimization can be reduced by following more packets. However, the computer times start to get excessive if this is the only approach used. It would be more fruitful in terms of the routine application of the program to expend some effort towards altering the importance sampling.

The FASTER-III program has the capability of calculating optimal importance parameters based on partial derivatives of the variance. This feature can be used in determining better importance sampling parameters for shield optimization problems. In fact, the overall program efficiency could be improved if this feature was utilized on a wide variety of problems with the results being used to improve the built-in importance sampling models and parameters.

The relative expense of using the FASTER-III program in a somewhat iterative fashion to do the initial sizing of a shield configuration should be considered. The least expensive procedure suggested for the initial setup of a problem would involve either hand calculations and/or point kernel calculations. In view of this sizing problem, it is recommended that a point kernel option -- removal and/or moments data for neutrons, buildup factors for photons -- be built into the FASTER-III program. This option would also include a calculation of secondary photon contributions. This option could be used in conjunction with the shield optimization procedure and permit relatively accurate sizing with an order of magnitude or more reduction in computer time when compared with the use of Monte Carlo. A very positive advantage of this option is that most of the data cards used in a point kernel problem would be used directly in the corresponding Monte Carlo problem. The incorporation of a point kernel option in the FASTER-III program does not involve very major modifications. In fact, a similar option was used in one modification of the original FASTER program for calculating secondary photon dose rates.

REFERENCES

1. Jordan, T. M., "FASTER, A Fortran Analytical Solution of the Transport Equation by Random Sampling", Synthesis of Computational Methods for the Design and Analysis of Radiation Shields for Nuclear Rocket Systems, Vol. 9, Westinghouse Report WANL-PR-(LL)-010, June 1967.
2. Jordan, T. M., BETA, A Monte Carlo Computer Program for Bremsstrahlung and Electron Transport Analysis, AFWL-TR-68-111, October 1968.
3. Jordan, T. M., Non-Negative Multigroup Cross Sections for FASTER, A.R.T. Research Corporation Report No. ART-19, September 1968.
4. Jordan, T. M., and M. L. Wohl, Helical Duct Geometry Routine for the Shielding Computer Program FASTER, NASA TM X-1838, 1969.
5. Jordan, T. M., "Advanced Monte Carlo Concepts-Methods and Applications", Trans. Am. Nucl. Soc., 12, 945, (1969).
6. Jordan, T. M., FASTER, A Generalized-Geometry Monte Carlo Computer Program for the Transport of Neutrons and Gamma Rays (Revised Version), Volume I - Summary Report, A.R.T. Research Corporation Report No. ART-42, June 1970.
7. E. S. Troubetzkoy and M. L. Wohl, UNAMIT-A One Dimensional 4 Pi Spherical Multilayer Reactor-Shield-Weight Optimization Code, NASA TM X-2048, July 1970.
8. Wohl, M. L., Private Communication, December 3, 1970.

Appendix A
MONTE CARLO METHOD

The Monte Carlo method as used in the FASTER program is described in this appendix. The development starts with the order-of-scatter (Neumann series) solution of the transport equation. The Monte Carlo method is then applied to the spatial integrations. The presentation is of a summary nature and no proofs are given.

1. The Transport Equation

The particle energy is immediately cast into a multigroup framework where the ith energy group includes all particles with energies E between the group boundaries E_i and E_{i+1} . In the conventional manner, higher group indices will indicate lower particle energies, i.e., the energy group boundaries are monotonically decreasing, $E_i \geq E_{i+1}$.

The differential angular source of particles in the ith energy group which have had exactly k interactions or collisions since being emitted from a known independent source is denoted by $S_{ik}(\underline{x}, \underline{u})$, the number of particles in group i per cm^3 per steradian coming out of a collision at \underline{x} and proceeding in the direction \underline{u} .

The differential angular flux of particles in the jth energy group due to source particles which have had k collisions is denoted by $\phi_{jk}(\underline{y}, \underline{v})$, the number of particles in group j per cm^2 per steradian crossing a detector at \underline{y} while heading in the direction \underline{v} .

The differential angular flux is directly related to the differential angular source by a simple line integral over the space points which can contribute in the fixed direction \underline{v} .

Allowing for the application of this development to charged particle transport, the relationship between flux and source is written as:

$$\phi_{jk}(\underline{y}, \underline{v}) = \sum_i \int_0^{\infty} S_{ik}(\underline{y}-t\underline{v}, \underline{v}) K_{ij}(\underline{y}-t\underline{v}, \underline{y}) dt \quad (A1)$$

In general, the kernel $K_{ij}(\underline{x}, \underline{y})$ is the probability that a particle starting at \underline{x} in group i will arrive at \underline{y} in energy group j . For neutral particle transport, this kernel is simply:

$$K_{ij}(\underline{x}, \underline{y}) = \exp \left[- \int_0^t \Sigma_i(\underline{x}+s\underline{u}) ds \right] \delta_{ij} \quad (A2)$$

$$t = |\underline{y}-\underline{x}|, \quad \underline{u} = (\underline{y}-\underline{x})/t$$

where $\Sigma_i(\underline{z})$ is an appropriately averaged total cross section for energy group i at the point \underline{z} . The quantity δ_{ij} is the Kronecker delta function, $\delta_{ij} = 0$ if $i \neq j$, $\delta_{ij} = 1$ if $i = j$.

The "next collision" angular source, $S_{i,k+1}(\underline{x}, \underline{u})$, is, in turn, determined from the angular flux as:

$$S_{i,k+1}(\underline{x}, \underline{u}) = \sum_j \int_{4\pi} \phi_{jk}(\underline{x}, \underline{v}) T_{ji}(\underline{x}, \underline{u}, \underline{v}) d^2\underline{v} \quad (A3)$$

This calculation requires an integration over all initial directions \underline{v} (differential solid angle $d\Omega = d^2\underline{v}$) which can be scattered into the direction \underline{u} . A summation over all initial

groups j for which particles can scatter into group i is also required. The kernel $T_{ji}(\underline{x}, \mu)$ is the probability per unit path length per steradian that a particle at \underline{x} will scatter from group j into group i while being deflected through an angle $\cos^{-1} \mu$.

2. Monte Carlo Integration

The Monte Carlo method is used to reduce the integrations above to one-point numerical quadratures where the point is selected at random. Assuming the most desirable solution is represented by the scalar flux at a specified point \underline{y} , then this point solution is composed of contributions from the many orders-of-scatter:

$$\phi_j(\underline{y}) = \sum_k \phi_{jk}(\underline{y}) \quad (A4)$$

where $\phi_{jk}(\underline{y})$ is the scalar flux in group j at \underline{y} from particles which have had exactly k collisions. Each order-of-scatter component of the flux can be written as volume integration over the k th scattered source since:

$$\phi_{jk}(\underline{y}) = \int_{4\pi} \phi_{jk}(\underline{y}, \underline{v}) d^2 \underline{v} \quad (A5)$$

$$= \int_{4\pi} \left\{ \sum_i \int_0^\infty S_{ik}(\underline{y}-t\underline{v}, \underline{v}) K_{ij}(\underline{y}-t\underline{v}, \underline{y}) dt \right\} d^2 \underline{v} \quad (A6)$$

$$= \int_{4\pi} \int_0^\infty \sum_i S_{ik}(\underline{y}-t\underline{v}, \underline{v}) K_{ij}(\underline{y}-t\underline{v}, \underline{y}) \frac{1}{t^2} t^2 dt d^2 \underline{v} \quad (A7)$$

The differential volume element $t^2 dt d^2 \underline{v}$ is written in the more general form $d^3 \underline{x}$ where \underline{x} represents the space point $\underline{y} - t\underline{v}$. The directionality of the source is changed from \underline{v} to the more general \underline{u} by including an appropriate delta function in the integrand. The final form of the equation for the k th scattered flux in group j at \underline{y} is:

$$\phi_{jk}(\underline{y}) = \sum_i \int S_{ik}(\underline{x}, \underline{u}) K_{ij}(\underline{x}, \underline{y}) \frac{\delta(\underline{u} - \underline{v})}{t^2} d^3 \underline{x} \quad (\text{A8})$$

$$t = |\underline{y} - \underline{x}|, \quad \underline{v} = (\underline{y} - \underline{x})/t$$

This equation is unchanged if the integrand is multiplied and divided by the probability density function (pdf) $p_k^*(\underline{x})$:

$$\phi_{jk}(\underline{y}) = \int \sum_i \left\{ \frac{S_{ik}(\underline{x}, \underline{u})}{p_k^*(\underline{x})} \right\} \left\{ K_{ij}(\underline{x}, \underline{y}) \frac{\delta(\underline{u} - \underline{v})}{t^2} \right\} p_k^*(\underline{x}) d^3 \underline{x} \quad (\text{A9})$$

where

$$p_k^*(\underline{x}) \geq 0 \quad \text{for all } \underline{x} \quad (\text{A10})$$

$$p_k^*(\underline{x}) > 0 \quad \text{if} \quad \sum_i \int_{4\pi} S_{ik}(\underline{x}, \underline{u}) d^2 \underline{u} > 0 \quad (\text{A11})$$

$$\int p_k^*(\underline{x}) d^3 \underline{x} = 1 \quad (\text{A12})$$

Equations A10 and A12 are necessary conditions in defining a pdf; it must be non-negative and must integrate to unity. The condition in equation A11 is stronger than is required for calculating the flux at \underline{y} -- as written, the same pdf can be used for calculating the $(k+1)$ th scattered source for the next order scalar flux component.

The quantity in the first set of brackets in the integrand of equation A9 represents a modified source density denoted by:

$$S_{ik}^*(\underline{x}, \underline{u}) = \frac{S_{ik}(\underline{x}, \underline{u})}{p_k^*(\underline{x})} \quad (A13)$$

The second bracketed quantity in equation A9 depends on the particular point \underline{y} at which the scalar flux is being calculated.

Equation A9 is integrated by selecting a single point \underline{z}_k at random from the probability density function $p_k^*(\underline{x})$. The mechanics of the random selection process will not be discussed here. It suffices for this discussion that a value \underline{x}_k , obtained at random from $p_k^*(\underline{x})$, gives a one point quadrature estimate of the value of the integral in equation A9. This estimate is denoted by $\phi_{jk}(\underline{y})$ and is given by

$$\phi_{jk}(\underline{y}) = \sum_i S_{ik}^*(\underline{z}_k, \underline{u}) K_{ij}(\underline{z}_k, \underline{y}) \frac{\delta(\underline{u} - \underline{v}_k)}{t_k^2} \quad (A14)$$

$$t_k = |\underline{y} - \underline{z}_k|, \quad \underline{v}_k = (\underline{y} - \underline{z}_k)/t_k$$

Of particular interest is the fact that equation A14 holds for all detector positions \underline{y} and all energy groups j . It is true that there is a particular pdf $p_k^*(\underline{x})$ that is best for calculating the k th scattered scalar flux in group j at \underline{y} , namely

$$p_k^*(\underline{x}) = \frac{\sum_i S_{ik}(\underline{x}, \underline{u}) \frac{K_{ij}(\underline{x}, \underline{y}) \delta(\underline{u} - \underline{v}_k)}{t^2}}{\int \sum_i S_{ik}(\underline{x}, \underline{u}) \frac{K_{ij}(\underline{x}, \underline{y}) \delta(\underline{u} - \underline{v}_k)}{t^2} d^3 \underline{x}} \quad (\text{A15})$$

Sampling of this pdf to obtain the discrete point \underline{z}_k will give an exact solution for the k th scattered scalar flux in group j at \underline{y} . However, there are several reasons for not doing so. Foremost is the fact that in defining the pdf through equation A15 it is necessary to essentially calculate the flux analytically since the denominator is the desired answer. Second, it is virtually impossible to define and then sample a pdf as complicated as equation A15. Furthermore, it is usually more economical to approximate equation A15 for the dominant energy group and then use the selected point \underline{z}_k in the calculation of fluxes for all the energy groups simultaneously as implied in equation A14. Finally, this optimal pdf only holds for the k th scattered flux, and the next step after calculating the k th scattered flux is to use the source strengths $S_{ik}(\underline{z}_k, \underline{u})$ in defining the $(k+1)$ th scattered source for the next order of scatter. There is a different and much more complicated prescription for defining an optimal pdf to be used in the selection of \underline{z}_k for this next step.

After these negative comments, there are several features of equation A15 which are quite useful. It does provide insight

into the functional form of the optimum last collision probability density function. Furthermore, the more complex pdf to be used for future orders-of-scatter can be approximated by equation A15 by simple alterations of the transport kernel $K_{ij}(\underline{x}, \underline{y})$. Finally, it does include the $1/t^2$ singularity in a manner which obviates any difficulties in calculating accurate, finite variance fluxes at a point.

As discussed above, the pdf $p_k^*(\underline{x})$ is used to select a discrete point \underline{z}_k which is then used via equation A14 to estimate scalar fluxes at the point \underline{y} . The point source defined at \underline{z}_k can actually be used in the estimate of angular fluxes since the source strengths $S_{ik}^*(\underline{z}_k, \underline{u})$ can be evaluated for various directions. Thus, the angular flux at any point \underline{y} can be estimated, using these same sources, as:

$$\phi_{jk}(\underline{y}, \underline{v}) = \sum_i S_{ik}^*(\underline{z}_k, \underline{v}) \frac{K_{ij}(\underline{z}_k, \underline{x}) \delta(\underline{v} - \underline{v}_k)}{t_k^2} \quad (\text{A16})$$

$$t_k = |\underline{y} - \underline{z}_k| \quad , \quad \underline{v}_k = (\underline{y} - \underline{z}_k) / t_k$$

Of course, if the point \underline{y} lies in the k th scattered source volume, a pdf which includes a dependence on \underline{y} should be used in selecting \underline{z}_k . However, if \underline{y} lies outside this source volume, there is no difficulty.

In addition, these point value flux estimates can be area or volume averaged. The equations are simply

$$\phi_{jk}(A, \underline{v}) = \sum_i \frac{1}{A} \int_A S_{ik}^*(\underline{z}_k, \underline{v}) K_{ij}(\underline{z}_k, \underline{v}) \frac{\delta(\underline{v} - \underline{v}_k)}{t_k^2} dA \quad (A17)$$

$$\text{and } \phi_{ik}(V, \underline{v}) = \sum_i \frac{1}{V} \int_V S_{ik}^*(\underline{z}_k, \underline{v}) K_{ij}(\underline{z}_k, \underline{v}) \frac{\delta(\underline{v} - \underline{v}_k)}{t_k^2} dV \quad (A18)$$

In both cases, the integrations are transformed to spherical coordinates so that $dA = t_k^2 \frac{d^2 \underline{v}_k}{|\underline{v}_k \cdot \underline{n}|}$ where \underline{n} is the normal to

the area, and $dV = t_k^2 d^2 \underline{v}_k dt_k$ so that

$$\begin{aligned} \phi_{jk}(A, \underline{v}) &= \sum_i \frac{1}{A} \int_{4\pi} S_{ik}^*(\underline{z}_k, \underline{v}) K_{ij}(\underline{z}_k, \underline{z}_k + t_k(\underline{v})) \frac{\delta(\underline{v} - \underline{v}_k) t^2 d^2 \underline{v}_k}{t_k^2 |\underline{v}_k \cdot \underline{n}|} \\ &= \sum_i \frac{1}{A} S_{ik}^*(\underline{z}_k, \underline{v}) \frac{K_{ij}(\underline{z}_k, \underline{z}_k + t_k(\underline{v}))}{|\underline{v}_k \cdot \underline{n}|} \end{aligned} \quad (A19)$$

$$\phi_{ik}(V, \underline{v}) = \sum_i \frac{1}{V} \int_{4\pi} \int_{t_k(\underline{v})}^{\tau_k(\underline{v})} S_{ik}^*(\underline{z}_k, \underline{v}) K_{ij}(\underline{z}_k, \underline{z}_k + t_k \underline{v}) \frac{\delta(\underline{v} - \underline{v}_k)}{t_k^2} t_k^2 d^2 \underline{v}_k dt_k$$

$$= \sum_i \frac{1}{V} S_{ik}^*(\underline{z}_k, \underline{v}) \int_{t_k(\underline{v})}^{\tau_k(\underline{v})} K_{ik}(\underline{z}_k, \underline{z}_k + t_k \underline{v}) dt_k \quad (\text{A20})$$

where $t_k(\underline{v})$ is the distance from \underline{z}_k along \underline{v} up to the area or volume, and $\tau_k(\underline{v})$ is the distance through the volume. Any summations over multiple intersections of the line $\underline{z}_k + t_k \underline{v}$ with the area or volume are implicit in the above equations.

The point angular fluxes defined by equation A16 are used to define the $(k+1)$ th scattered source:

$$S_{i,k+1}(\underline{x}, \underline{u}) = \sum_j \int_{4\pi} \phi_{jk}(\underline{x}, \underline{v}) T_{ji}(\underline{x}, \underline{v} \cdot \underline{u}) d^2 \underline{v} \quad (\text{A21})$$

This reduces to:

$$S_{i,k+1}(\underline{x}, \underline{u}) = \sum_j \phi_{jk}(\underline{x}, \underline{v}_k) T_{ji}(\underline{x}, \underline{v}_k \cdot \underline{u}), \quad (\text{A22})$$

since the angular fluxes are defined as being in the direction \underline{v}_k only, where $\underline{v}_k = (\underline{x} - \underline{z}_k) / |\underline{x} - \underline{z}_k|$.

As before, a pdf, $p_{k+1}^*(\underline{x})$, the $(k+1)$ th source is defined and then sampled to obtain a discrete value \underline{z}_{k+1} of \underline{x} . The source strength at this point is then denoted by $S_{i,k+1}^*(\underline{z}_{k+1}, \underline{u})$ and is given by

$$S_{i,k+1}^*(\underline{z}_{k+1}, \underline{u}) = \frac{S_{i,k+1}(\underline{z}_{k+1}, \underline{u})}{p_{k+1}^*(\underline{z}_{k+1})} \quad (\text{A23})$$

$$= \sum_j \frac{\phi_{jk}(\underline{z}_{k+1}, \underline{v}_k)}{p_{k+1}^*(\underline{z}_{k+1})} T_{ji}(\underline{z}_{k+1}, \underline{v}_k \cdot \underline{u}) \quad (\text{A24})$$

Since flux estimates may require evaluation of $S_{i,k+1}^*(\underline{z}_{k+1}, \underline{u})$ for various directions \underline{u} , it is expedient to define point mono-directional values of the flux going into the point \underline{z}_{k+1} :

$$\phi_{jk}^*(\underline{z}_{k+1}, \underline{v}_k) = \frac{\phi_{jk}(\underline{z}_{k+1}, \underline{v}_k)}{p_{k+1}^*(\underline{z}_{k+1})} \quad (\text{A25})$$

The angular point source $S_{i,0}^*(\underline{z}_{k+1}, \underline{u})$ is determined from input only for the independent source. In all other instances, it is determined from the equation

$$S_{i,k+1}^*(\underline{z}_{k+1}, \underline{u}) = \sum_j \phi_{jk}^*(\underline{z}_{k+1}, \underline{v}_k) T_{ij}(\underline{z}_{k+1}, \underline{v}_k \cdot \underline{u}) \quad (\text{A26})$$

The process of reducing each volume-distributed order-of-scatter source to a point representation by random sampling, of using the same point representation to give the volume-distributed source for the next order of scatter is continued until all the particles at a given order of scatter no longer yield a

significant contribution to the flux estimates. The estimate of the total angular flux at a point \underline{y} from this procedure is then obtained by summing the individual order-of-scatter components:

$$\phi_j(\underline{y}, \underline{v}) = \sum_k \phi_{jk}(\underline{y}, \underline{v}) \quad (\text{A27})$$

$$= \sum_k \sum_i S_{ik}^*(\underline{z}_k, \underline{v}) \frac{K_{ij}(\underline{z}_k, \underline{y})}{t_k^2} \delta(\underline{v} - \underline{v}_k) \quad (\text{A28})$$

The total scalar flux is obtained by a simple integration over solid angle which yields

$$\phi_j(\underline{y}) = \sum_k \sum_i S_{ik}^*(\underline{z}_k, \underline{v}_k) \frac{K_{ij}(\underline{z}_k, \underline{y})}{t_k^2} \quad (\text{A29})$$

This process gives a single, inaccurate, estimate of the total flux. Therefore the process is repeated a specified number of times and the average of all the estimates is accepted as the best estimate of the total flux. Introducing the subscript n to denote the iteration index, then $\phi_{jn}(\underline{y})$ is the estimate of the flux in the j th energy group at \underline{y} of particles obtained on the n th iteration. If N is the total number of iterations, then the total flux is estimated by:

$$\bar{\phi}_j(\underline{y}) = \frac{1}{N} \sum_{n=1}^N \phi_{jn}(\underline{y}) \quad (\text{A30})$$

Since each iterant represents an independent estimate of the flux, it is possible to approximate the standard deviation of the total flux by:

$$\sigma_j(\underline{y}) = \left[\frac{1}{N-1} \left\{ \frac{1}{N} \sum_{n=1}^N \phi_{jn}^2(\underline{y}) - \bar{\phi}_j^2(\underline{y}) \right\} \right]^{\frac{1}{2}} \quad (\text{A31})$$